Initial stages of oxygen adsorption on Si(111): The stable state

P. Morgen,* U. Höfer, W. Wurth, and E. Umbach†
Physik-Department (E-20), Technische Universität München, D-8046 Garching bei München, West Germany
(Received 22 May 1988)

We present new experimental results from a comprehensive study of the chemisorption of oxygen on differently prepared Si(111) surfaces, using low-energy electron diffraction and high-resolution electron spectroscopies such as x-ray photoemission spectroscopy, x-ray-initiated Auger-electron spectroscopy, and polarization-dependent ultraviolet photoemission spectroscopy. In the monolayer regime two different states of oxygen have been observed: a molecular precursor and a stable dissociated configuration. The latter is the subject of this paper. Its electronic structure and local symmetry are compatible only with a bridge-bonded atom between Si atoms in the first and second layer, respectively, with relatively little influence on the dangling bonds. The presence of a second dissociated oxygen adsorbate, e.g., a diatomiclike monoxide, is excluded by our data. The coverage dependent O 1*s* and Si 2*p* data indicate that the observed satellite structures in the submonolayer regime are due to excitations rather than to chemically shifted peaks from atoms in different bonding situations.

I. INTRODUCTION

The mechanism of oxygen adsorption on semiconductors as a first step of oxidation, and the identification of the bonding configurations of oxygen during this stage of adsorption, remain questions of central interest in surface science,[1] and largely unsolved.[2,3] As still more experimental results are published with improved experimental techniques,[3–7] or those based on comparisons with refined theoretical treatments,[8] the older literature is found to contain a number of hypothetical conclusions, where methods and data were, in fact, insufficient. It also appears that the most commonly applied surface-sensitive spectroscopies, such as Auger-electron spectroscopy (AES), ultraviolet photoemission spectroscopy (UPS), x-ray photoemission spectroscopy (XPS), and low-energy electron-loss spectroscopy with high resolution (HREELS), have some inherent biases the way they are commonly practiced, in particular when, essentially, a single technique is applied. Moreover, sample preparation and oxygen exposure conditions may be found to vary strongly between different reports, and claims as to the reproducibility of the results were not always substantiated.

A large interest has centered on the case of oxygen adsorption on silicon surfaces in an attempt to understand the manageable properties of the Si/SiO_2 interface, which is the key to the very successful silicon metal-oxide-semiconductor (MOS) technology.[9] However, it is generally agreed that clean silicon surfaces cannot be directly oxidized to form thick bulklike SiO_2 overlayers by exposure to dry, unexcited oxygen at room temperature. The reason is that the initially adsorbing oxygen molecules, under these conditions, saturate the surface with an oxygen species which must be energetically and/or sterically blocking any further uptake of oxygen at and through the surface. To identify this oxygen species and its configuration has been the subject of many studies,[1–8,10–15] using surface-sensitive spectroscopies with sensitivities typically down to a few percent of monolayer coverage. Different silicon surfaces with different stable surface reconstructions or different degrees of surface disorder have been studied,[7] with the result that differences in reactivity with respect to oxygen have been unraveled.

In the present investigation we have attempted to provide an extensive, complementary set of data for the interaction of oxygen with the Si(111) surface at low coverages. A particular advantage of the present approach, as compared to various previous publications, is the combination of many results obtained by *different* techniques under closely controlled *identical* conditions for a variety of parameters such as surface structure, oxygen exposure, and substrate temperature. In particular, surface techniques such as angle-dependent, high-resolution XPS (valence levels, O 2*s*, Si 2*p*, *and* O 1*s*), polarization and angle-dependent UPS, as well as high-resolution, x-ray-initiated AES (XAES) were combined to compare the different results from identical surfaces. Low-energy electron diffraction (LEED) was employed to study the surface structure and perfection during preparation of the silicon surfaces and as a result of various oxygen exposures. We studied oxygen adsorption on atomically clean surfaces and on surfaces with a controlled amount of foreign atoms (Ni and C), and we prepared various surface structures, as characterized by their LEED patterns: [7×7], [1×1], "[1×1]";(Ni), and completely disordered sputtered surfaces.

Our previous experiments[7] on the kinetics of oxygen adsorption at room temperature on differently prepared surfaces showed that for all Si(111) surfaces studied the sticking probability for oxygen decreases rapidly during buildup of the first layer. The initial sticking probability as well as the amount of adsorbed oxygen after identical doses are highest for a clean [7×7] surface and lowest for a sputtered, disordered surface.[7] The results confirm the earlier finding[10] of a fast initial adsorption stage fol-

lowed by a slower sorption process.

Our present investigations were performed to detect possible differences in the atomic and electronic structure of the silicon surfaces with adsorbed oxygen in these two initial stages of adsorption. The most notable result is the discovery of a *metastable molecular-oxygen* species,[11–13] most likely a peroxy bridge molecule, as an intermediate in the chemisorption process or, more accurately, a precursor to the stable dissociated oxygen adsorbate. The lifetime of this precursor was found to depend on temperature, probing radiation, oxygen exposure, impurities, and surface structure.[11,13] It thus appeared with variable relative intensities and time dependences in our various measurements, and probably elsewhere too, making its appearance difficult to ascertain.[3,14,15] However, once its spectroscopic features are recognized, its influence on the spectra of mixed layers can be determined and the spectra correspondingly corrected to allow a discussion of the characteristics of the stable chemisorbed oxygen species. The precursor results, in particular, its characterization and decay kinetics, and the influence of the substrate will be discussed in detail in the following paper.[13]

In this paper we concentrate on the *stable oxygen species* which is the decay product of the precursor, or, in general, the stable reaction product of oxygen chemisorption on clean or adsorbate (e.g., O, C or Ni) covered silicon surfaces. We show that the stable species is an atomic configuration, i.e., oxygen is dissociatively adsorbed. All of our results including the comparison of our angle- and polarization-dependent UPS data with theoretical calculations are fully consistent with a bridge-bonded O configuration in a short bridge between Si atoms (silicon monoxide), as proposed earlier.[4] The influence of surface structure and cleanliness on adsorption kinetics and spectral features is remarkable and will be discussed together with the role of the dangling bonds observed in UPS. The high-resolution core-level spectra show additional structures which were previously interpreted as different formal oxidation states of silicon (Si $2p$ spectra) and diatomic silicon monoxide species (O $1s$ spectra), respectively. We object to the interpretation of a diatomiclike monoxide at low or medium exposures, and we tentatively suggest excitonic and interband excitations rather than intermediate oxidation states as explanation of the high-energy structures in the low-coverage regime.

The structure of this paper is as follows. The description of the experimental conditions in Sec. II is followed by a section with the presentation and discussion of the results (Sec. III). Then follows a general discussion of the stable oxygen state(s), including a comparison with theory, and an alternative interpretation of the additional spectral features (Sec. IV). A summary of the results (Sec. V) concludes the paper.

II. EXPERIMENTAL METHODS

The silicon crystals used were n-type [$n(\mathrm{P}) \sim 10^{17}$ cm^{-3}] from Wacker Chemitronic. Samples with (111) surfaces were prepared by cutting (111)-oriented silicon wafers into squares of approximately 1×1 cm^2 ($\times 0.2$ cm thickness) and by orienting and polishing them. The sample holder was fitted with two W wires engaging grooves notched into two of the sides of the crystals. A chromel/alumel thermocouple was spotwelded to one of the W wires, close to the crystal. Uniform heating was obtained by bombarding the back side of the crystal with electrons from a separate, moveable filament, with a bias applied to the crystal. Cooling facilities were also provided in the form of a liquid-nitrogen bath in thermal contact with the W wires. The samples could be transferred in and out of the ultrahigh vacuum chamber through a fast entry system. The final processing of samples was done inside the chamber. It always included many cycles of oxygen treatment and sputtering with 600 eV Ar^+ ions, normally followed by annealing.

The experimental facilities consist of a modified Vacuum Generators (VG) ESCALAB-Mk I system, equipped with a twin anode (Mg, Al) x-ray source, an x-ray monochromator, a spherical (150°) sector analyzer with a position sensitive detector array at the output focal plane for high sensitivity and energy resolution, and with a transfer lens between sample and analyzer with variable input aperture for selecting high sensitivity or high-angular resolution. Further equipment includes a high-flux uv lamp (Vactronic) with polarizer for He I light (VG), LEED optics (Riber), and a gas dosing system.

The gas doser is a glass capillary array, suspended over the crystal surface to direct a homogeneous current of effusing gas particles onto the surface. The inlet system consists of differently sized volumes which are separated from the main gas supply and the glass capillary array with right angle toggle valves. To obtain a given exposure, one of these volumes is filled with oxygen at a selected pressure, and is then dosed onto the sample through the glass capillaries. This procedure allows us to achieve very reproducible gas doses (1–5 %, depending on the pressure needed in the supply volume). Optimally clean conditions for the gas exposures are assured by a short distance between gas doser and crystal and by a good base pressure ($\leq 5 \times 10^{-11}$ mbar). As a further precaution, the ionization gauge was always turned off during exposures. Note also that the system is pumped by diffusion pumps, so that there is no possibility of getting oxygen excited by ion pumps.

The electron spectrometer was calibrated (accuracy ~ 50 meV), in agreement with standards set down by the National Physics Laboratory (Teddington, United Kingdom),[16] and controlled by a microprocessor based data acquisition system. Some of the data were treated by mathematical methods such as Fourier smoothing, spin-orbit decomposition, and deconvolution,[17] which will be described in more detail in the following paper.[13] In most cases smoothed curves as well as original data points are shown.

The differently prepared Si(111) surfaces of this study were [7×7] surfaces with variable amounts of C impurities (0–5 %), including virtually clean surfaces, a clean [1×1] surface produced by Ar^+ bombarding (600 eV) followed by mild annealing to desorb Ar, a "[1×1]" surface stabilized by small amounts of Ni (about 3–5 % in

the surface region, as derived from XPS), and an Ar^+ sputtered, totally disordered surface. For comparison, data from a SiO_2 sample were also taken. The SiO_2 sample was a chemically grown, $\simeq$100-nm thick oxide film on a 0.2-mm thick silicon substrate.

III. EXPERIMENTAL RESULTS AND INTERPRETATION

In this section we present the experimental results grouped with respect to the techniques employed. References to previous experimental work are given for comparison, and some spectral features are discussed together with the presentation of the data. The conclusions drawn from the data as a whole are summarized in the general discussion of Sec. IV.

A. Si 2*p* and O 1*s* core lines

The Si 2*p* core lines excited with Mg $K\alpha$ radiation were recorded for various oxygen coverages on the different surfaces included in this study. The two major findings are first that there are no significant qualitative differences for the various surfaces, and secondly that the spectral region around the lines is only little affected by the oxygen exposures,[7] even after the highest doses employed (25 000 L O_2). [1 langmuir (L) $\equiv 10^{-6}$ Torr sec.] In particular, at grazing exit angles of the emitted photoelectrons, i.e., for conditions of high surface sensitivity, some shifted intensity is observable at the high-binding-energy side of the Si 2*p* peak (see Figs. 1 and 2). The details of this part of the spectrum are best recognized after stripping off the spin-orbit split $2p_{1/2}$ component and deconvoluting the instrumental broadening function.[13,17] The results of such a procedure are shown in Fig. 1 for one example, Si(111) [7×7] exposed to 250 L O_2. At the top, two spectra are displayed for normal and grazing emission angle, respectively. The dots represent original data points, the solid lines the result of a Fourier smooth. The middle spectrum shows the pure $2p_{3/2}$ component at grazing angles after stripping off the $2p_{1/2}$ peak, and the bottom spectrum is the (Fourier-smoothed) result of deconvoluting the measured instrumental function (Mg $K\alpha$ radiation plus analyzer transmission).[13,17]

The deconvoluted spectrum clearly shows a satellite at 0.9 eV higher binding energy (BE) which is already visible as a shoulder in the middle spectrum, and which reproducibly appears with varying intensity depending on oxygen coverage. The spectra also show some additional structures extending up to about 3.5 eV higher BE. Hollinger and Himpsel,[5,15] and subsequently others,[18–21] found very similar structures and distinguished peaks at 0.9, 1.8, 2.6, and 3.5 eV. They attributed these peaks to Si atoms in different bonding configurations and assigned them formally to Si^{1+}, Si^{2+}, Si^{3+} and Si^{4+}. We have indicated their peak positions in Fig. 1 by marks but we note that positions *and* intensities of our peaks between 1.8 and 3.5 eV depend on coverage, signal-to-noise ratio, and deconvolution procedure. Hence one cannot claim to be able to discern "peaks" or satellites, apart from that at 0.9 eV, in the coverage range studied here. This statement is also true for the spin-orbit decomposed spectra of Fig. 2 obtained after different oxygen exposures. We note, however, that a peak at 3.5–4 eV higher binding energy does start growing at higher exposures (250–2500 L O_2) which remains weak for dry oxygen exposures but increases drastically for thermally grown oxide films.[5] This peak indicates the growth of amorphous silicon dioxide and shifts gradually to higher binding energies. It appears at 5 eV higher BE for the SiO_2 sample (Fig. 2).

Next we consult the O 1*s* spectroscopic information. Figure 3 compares O 1*s* peaks recorded after different oxygen doses. The top spectrum shows SiO_2, the middle spectra represent two original O/Si(111)-[7×7] data sets both on the same intensity scale, whereas the bottom spectra were Fourier-smoothed, deconvoluted (instrumental function) and normalized to equal heights for better comparison of line-shape changes. These O 1*s* spectra, though 50% broader than the Si $2p_{3/2}$ spectra,

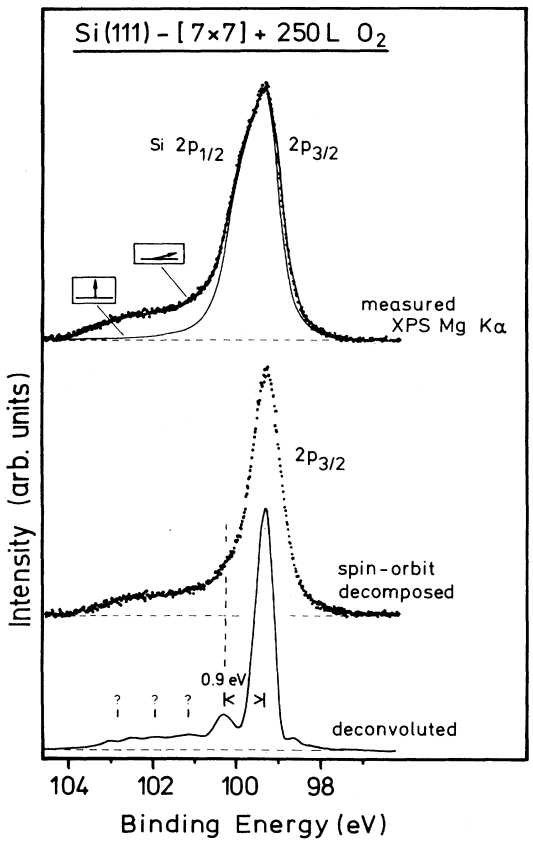

FIG. 1. Si 2*p* lines of a Si(111)-[7×7] surface exposed to 250 L O_2, as measured with Mg $K\alpha$ radiation (top), after stripping off the spin-orbit split $2p_{1/2}$ component (middle), and after deconvolution of an instrumental function which has been determined separately (bottom). Dotted curves represent original data points, solid lines are the result of Fourier smoothing (top) and deconvolution (bottom). The top spectra were taken at normal and grazing angles, respectively, in order to accentuate the contribution from the surface region.

also clearly show additional intensity on the high binding-energy side of the O 1*s* peak extending from 0.5 to about 3.5 eV energy separation. This intensity also grows with increasing exposure, perhaps showing some structure. We emphasize that no significant differences, i.e., differences beyond the noise level, could be observed between spectra taken at normal and grazing angle, respectively, at least not in the energy range within 3 eV from the peak maximum. This result indicates that the additional features are either satellites to the main peak or represent additional oxygen species with a depth distribution identical to that of the main component. We also note that the high-BE structures disappear upon heating to more than 500 °C.[6]

In the O 1*s* case, the comparison of results obtained from differently prepared surfaces reveals some lineshape differences. Even the raw data of Fig. 4 clearly indicate that the significant peak asymmetry of oxygen on the [7×7] surface, which is due to the additional structure at the high-binding-energy tail, is similar or slightly reduced for the [1×1];Ni surface but nearly disappears for the sputtered (disordered) Si surface (middle spectrum of Fig. 4). One could argue that the inhomogeneity of the sputtered surface leads to smearing of structures and asymmetry since different adsorption sites and bonding configurations may cause peak broadening. However, this effect must be rather small because the peak widths are nearly equal, and hence it cannot explain the disappearance of the asymmetry. In addition, the high-BE tail of the middle O 1*s* peak reaches less far than that of the bottom peak of Fig. 4.

In conclusion of this section we note that appealing, and by now apparently accepted, interpretations were previously given for the additional Si 2*p* and O 1*s* features. While the Si 2*p* structure is believed to contain distinct peaks representing Si atoms in different bond configurations with oxygen neighbors,[5,15,18–21] as mentioned above, the O 1*s* structure was explained as arising from diatomiclike silicon monoxide (Si=O).[6] We agree that the previous results gave good evidences for these interpretations, in particular, for the Si 2*p* structures in the high-coverage regime or for thermal oxide interfaces. We stress, however, that, at least in the low-coverage range, some doubts as to these interpretations arise. This is discussed in Sec. IV, and an alternative explanation for the additional structures as excitations is given. We are convinced that our data are more compatible with such a picture rather than with the earlier interpretation. Note that the presentation of our results and most of the conclusions are independent of this new interpretation.

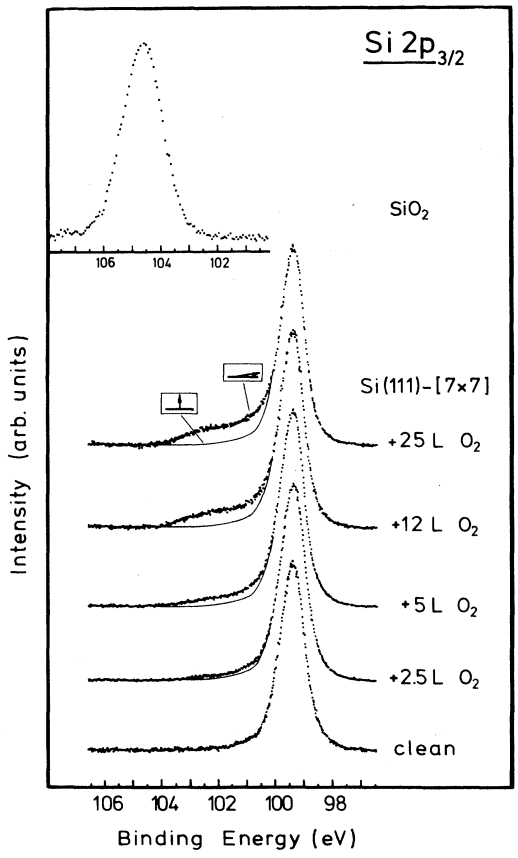

FIG. 2. Spin-orbit decomposed Si $2p_{3/2}$ spectra for SiO_2 and for various oxygen doses on Si(111)-[7×7] for normal (solid lines) and grazing (dots) emission angles.

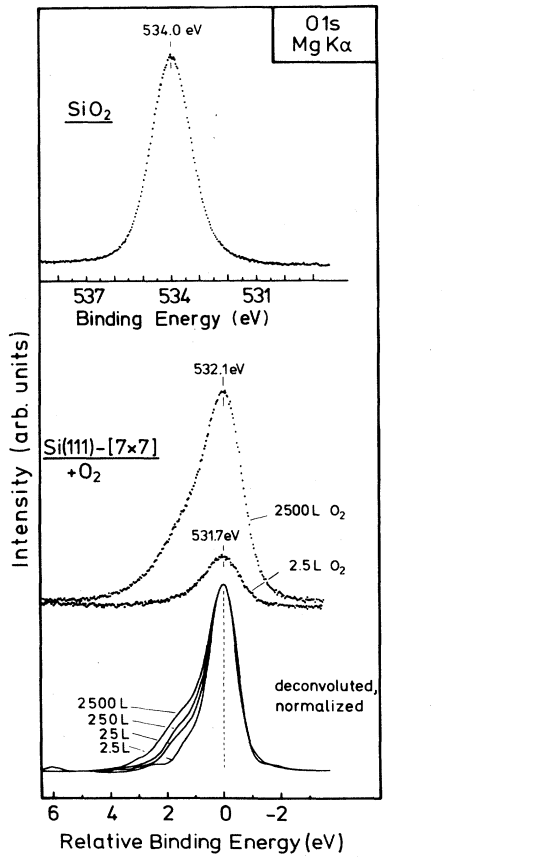

FIG. 3. Original O 1*s* spectra for SiO_2 (top) and for two different oxygen doses on Si(111)-[7×7] (middle) as well as Fourier-smoothed, deconvoluted, and normalized O 1*s* spectra, taken after four different exposures (bottom).

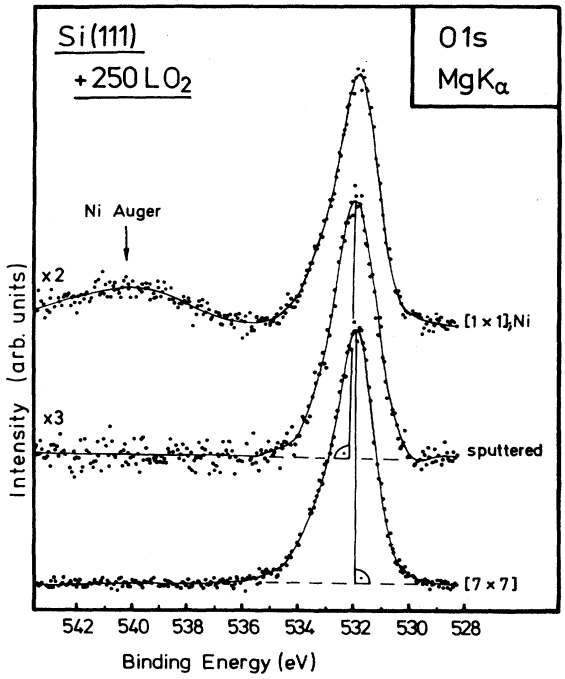

FIG. 4. Normalized O 1*s* spectra from differently prepared Si surfaces [7×7], sputtered, and [1×1];Ni obtained after equal exposures to 250 L O_2.

B. O *KLL* Auger spectra

X-ray-initiated Auger spectra (XAES) from the decay of an O 1*s* hole were recorded with high resolution and relatively good signal-to-noise ratios in the counting mode. Three spectra representing different oxygen coverages on the Si(111)-[7×7] surface are shown in Fig. 5 (middle). The spectra were Fourier-smoothed as indicated by the solid lines drawn through the original data points. Relevant oxygen Auger data from the literature are included in Fig. 5, such as isolated molecular O_2 (top),[22] SiO_2, as received and sputtered (middle), and oxygen adsorbed on W(110) (bottom).[23] The literature and SiO_2 data are shifted by several eV, as noted in the figure, in order to align with our O/Si data for ease of comparison. These shifts contain several contributions of different origins like different reference levels, chemical state, dynamical screening, effective hole-hole interaction in the Auger final state, etc.

The magnitude of the shift as well as the obvious differences between line shapes, relative peak positions, and intensities of our O/Si Auger spectra and those from molecular O_2 or O/W(110) make it clear that the latter represent different O-bonding situations. For instance, the obvious disagreement of the fingerprints from O/Si and molecular O_2 makes it unlikely that our stable oxygen species is molecularly adsorbed, since adsorbed species preserving their molecular integrity (e.g., CO, NO, N_2, N_2O) usually yield rather similar XAES spectra compared with the gas phase.[23] In fact, the results of a very recent study using synchrotron radiation clearly prove that the molecular precursor yields rather different Auger fine structures which resemble those of isolated O_2 (like the top spectrum of Fig. 5) and disagree with those of the present O/Si(111) data.[12] The difference between O/Si and O/W(110) is much less pronounced but still significant. This is understandable even if oxygen is atomically (dissociatively) bound to the surface in both cases, since the Si—O bond is much more covalent than the W—O bond.

The three O/Si spectra show only subtle differences which may not be significant in view of the poor S/N ratio of the "5 L" spectrum. The width of the prominent peaks seems to increase for higher coverages. The reason for this could be either increasing inhomogeneity in the

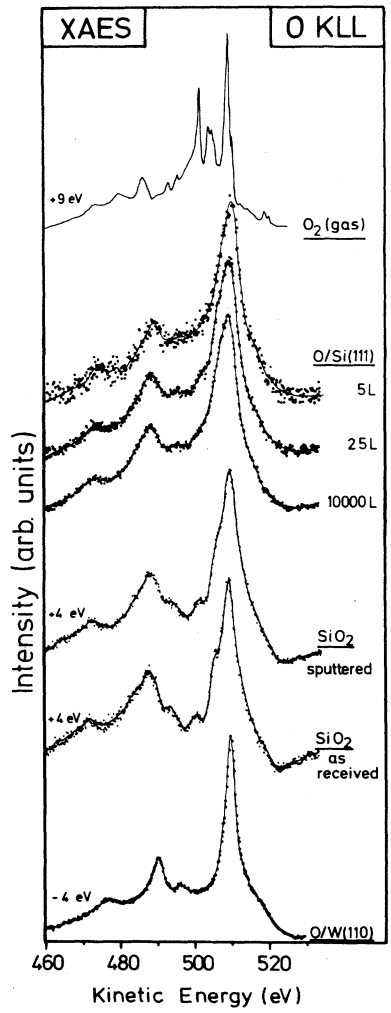

FIG. 5. Comparison of XAES spectra from O_2 gas (Ref. 22), oxygen adsorbed on Si(111)-[7×7] for three different doses, SiO_2 sputtered, SiO_2 as received, and dissociatively adsorbed oxygen on W(110) (Ref. 23). Note that the energy scale refers to O/Si(111), and that the other spectra were shifted by the energy values given in the figure. All energy scales refer to the Fermi level apart from that of gaseous O_2 which refers to the vacuum level.

surface region due to incorporation of oxygen, or additional, chemically different species, or excitations parallel to the Auger process like those discussed for the XPS peaks in Sec. IV C, or a combination of these effects. The apparent loss of resolution for the sputtered as compared to the "as received" SiO_2 sample (Fig. 5) supports the first suggestion.

It should be noted that the additional high-BE features observed in the *primary* photoionization (O 1*s*) spectra probably do not contribute to the Auger spectrum. Since these O 1*s* features appear on the high-BE side of the main O 1*s* peak they should, for instance, lead to enhanced emission on the high-kinetic-energy side of the main O *KLL* Auger peak at 510 eV, provided that no significant energy shifts occur, our new peaks appear, in the valence spectra, as in the present case (see below). This is apparently not the case because for increasing oxygen exposures no intensity increase could be found for the high-energy tail above 510 eV although the additional O 1*s* features grow considerably (compare Fig. 3). It could be argued that the Auger spectra of a different oxygen species, such as Si=O, may look rather different (e.g., with peaks below 510 eV only) thus explaining the missing intensity increase above 510 eV. However, careful analysis of the Auger line shapes of the high exposure spectra did not reveal *any* additional Auger features which are very likely to appear if a different oxygen species were added.

The explanation of the missing structure is very straightforward, however, if the high-BE O 1*s* features are satellites representing excitations. In this case additional Auger structures are not expected because most excited primary states settle down to the ionic ground state before the Auger decay occurs, as shown for several adsorbate systems.[24] Moreover, the increasing width and structure observed on the *low*-kinetic-energy side of the main Auger peaks would be consistent with excitations occuring during the Auger process.

Finally, we emphasize the striking similarity between the Auger line shapes of adsorbed O on Si and those of SiO_2. It is well established that the Auger decay is a very local process due to the nature of the two-electron matrix element. Thus the present *KLL* spectra display the local overlap of the valence (L) orbitals with the initial 1*s* (K) level which is localized around the oxygen nucleus. The similarity of the O/Si and SiO_2 Auger spectra then must indicate that the *local character* of the oxygen-derived orbitals is very similar for adsorbed oxygen at various coverages and for SiO_2. In any case, it proves that the stable oxygen adsorbate is dissociated at all coverages. A detailed discussion of the line shapes of SiO_2 and adsorbed O is given in Refs. 23 and 25.

C. He I and He II UPS spectra and polarization dependence

The valence electron structures of various silicon surfaces were studied with UPS using He I and He II radiation from a gas discharge lamp, and, in some cases, a polarizer for He I light. To assign structures in the UPS spectra due to adsorption of oxygen, and to assess the degree of structural information available from these spectra, a number of differently prepared Si(111) surfaces were studied as shown in Figs. 6–10. In these figures, all spectra are on the same intensity scale without any reduction or subtraction of background. The He I spectra were always recorded with a −15 volt bias applied to the crystal in order to reduce the influence of a small, residual magnetic field on the photoelectrons. A clean Ru surface was used to establish the location of the Fermi level, which is here used as the reference for binding energies. Spectra of the "clean" surface, i.e., the surface before oxygen adsorption, were also recorded; they are displayed at the bottom of each figure for reference. A comparison of the clean spectra from differently prepared surfaces will follow in our next paper[13] together with a discussion of the influence of the surface preparation on the adsorption behavior of the molecular precursor.

In the spectra of the *clean* Si(111)-[7×7] surface it is possible to assign a number of peaks, as indicated in Figs. 6 and 7 at positions which agree with published results. Peaks 1 and 2 are most likely due to surface states,[26] while peak 3 is due to a direct transition in the bulk.[27] Peaks 1 and 2 are also observed with He II radiation (Fig.

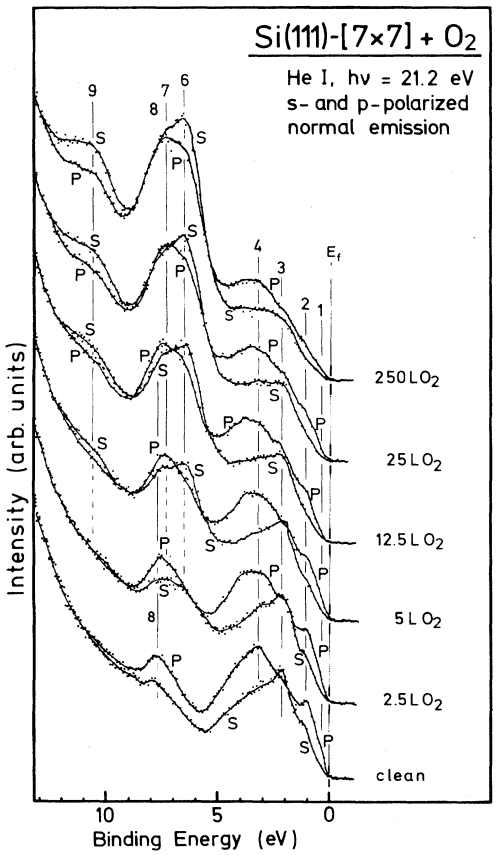

FIG. 6. Polarization-dependent He I UPS spectra for the clean and oxygen exposed Si(111)-[7×7] surface after various doses. Spectra taken with *s*- and *p*-polarized light are labeled by *S* and *P*, respectively. Prominent peaks and shoulders are labeled by numbers and are discussed in the text.

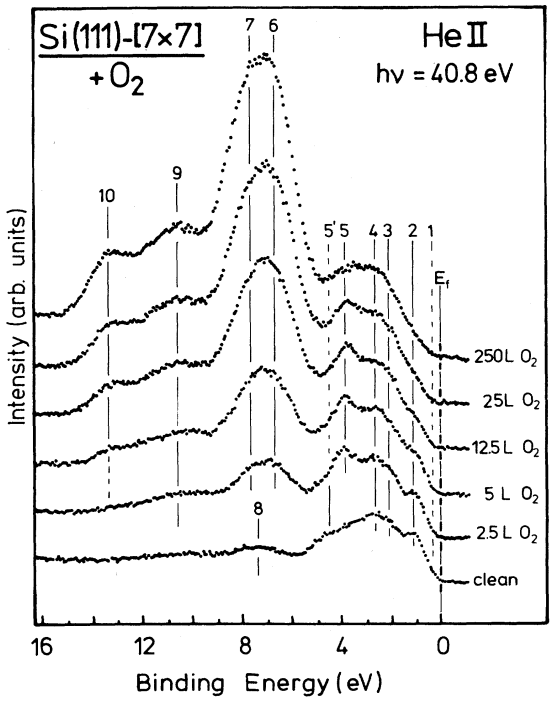

FIG. 7. He II UPS spectra from the clean and oxygen covered Si(111)-[7×7] surface.

7), while peak 3 is not. The symmetries of peaks 1 and 2, as observed with *s*-and *p*-polarized He I light (Fig. 6), agree with earlier findings,[26] allowing for the assignment of peak 2 as due to photoemission from the occupied dangling bonds since peak 2 is most pronounced for *p*-polarization indicating P_z symmetry. Peak 3, on the other hand, shows up for *s* polarization indicating P_{xy} symmetry. Since it disappears for increasing O coverage it could alternatively, or partly, be due to the Si backbonds. We note that after low oxygen exposures (≤ 10 L) an oxygen-derived peak which is due to the molecular precursor[11–13] appears at the same binding energy. The energies of the peaks are collected in Table I. Peak energies which are compatible with a (weak) structure in the respective spectrum but were derived from other data are denoted by parentheses.

The clean spectra from the Si(111)-[1×1], sputter-annealed surface (Figs. 8 and 9) look very similar to those from the [7×7] surface (Figs. 6 and 7) showing peaks at about the same binding energies. The only exception is the structure around 3.5 eV which is clearly a peak at 3 eV for the [7×7] surface but is smeared out for the [1×1] surface with a broad maximum at 3.8 eV in He I.

In Fig. 6 we also show a series of He I spectra of the [7×7] surface after *increasing oxygen exposures* obtained with two different polarizations. The geometry of the system allows the polarization vector to lie in the surface plane ("*s* polarization") or to be inclined at 30° to the normal ("*p* polarization"). The spectrometer accepted a narrow (1°) angular cone of emitted electrons around the normal to the surface. Oxygen exposure strongly affects the features in the upper part of the electron distribution (0–6 eV binding energies), including peaks 1–5. In addition, new peaks (6, 7, and 9) are seen to grow, with intensities scaling approximately with the O 1*s* signal (see later). Peaks 6 and 7 are here clearly distinguishable as two peaks, with different behavior with respect to polarization. The dangling bonds are affected by the adsorption of oxygen but are still clearly visible after 12.5 L, which corresponds to approximately 0.5 monolayers (see Fig. 12). At the highest coverage included here, the electron distribution from the Si valence band is relatively smooth and unstructured, probably due to a loss of order in the surface region and/or to scattering of the outgoing electrons. The LEED pattern in this case indicates that a large proportion of the surface layer is disordered.

A series of He II spectra of the [7×7] surface under conditions identical to those of Fig. 6 are shown in Fig. 7. Here, however, the resolution is set slightly lower than for the He I spectra in order to obtain a good signal-to-noise ratio. This could be the reason that the two peaks 6 and 7 are not well resolved in these spectra. A new

TABLE I. Binding energies (in eV) from He I and He II photoemission spectra of Si(111)-[7×7], referred to E_F.

	Peak number (referring to Figs. 6–10)									
Experiment	1	2	3	4	5,5	6	7	8	9	10
He I, clean surface	0.3	1.0	2.1	3.1	(3.8)			7.7		
He II, clean surface	(0.3)	1.1	(2.1)	2.7	(4.5)		7.3[a]	7.5[a]	10.1	
He I, average over 2.5, 5, 12.5, 25, and 250 L O_2	0.3[b]	1.0[c]	2.1[c,d]	3.2	3.9[d]	6.5	7.7[e]		10.7	
He II, average over 2.5, 5, 12.5, 25 and 250 L O_2		1.1[c]	(2.2)	3.0[f]	3.8[d]	7.4[a] 6.8[f]	7.7[f]		10.8	13.4[g]

[a]Composite peak.
[b]Only very weakly populated at 25 and 250 L O_2.
[c]Very weak at 250 L O_2.
[d]Molecular precursor.
[e]Very weak at 2.5 L O_2.
[f]After annealing at 400 K.
[g]Only seen for ≥ 5 L O_2.

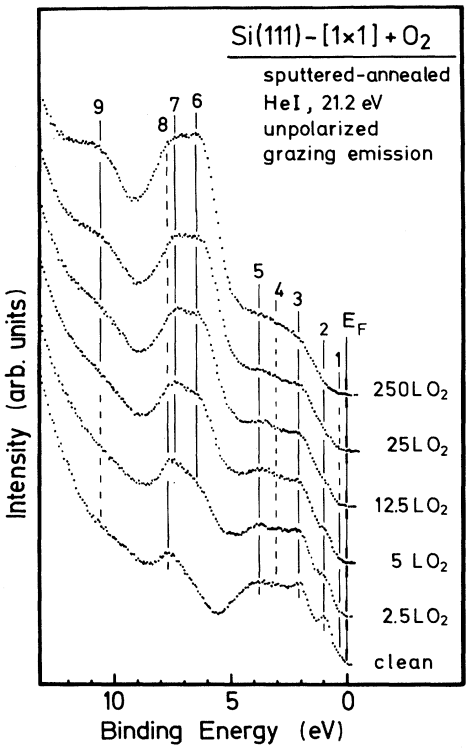

FIG. 8. Unpolarized He I UPS spectra from the clean and oxygen covered Si(111)-[1×1] surfaces prepared by sputtering and slight annealing.

feature, 10, is observed at higher binding energies than can be observed with He I radiation. The dangling bond peak (labeled 2) is vanishing gradually, as for He I.

A very interesting feature in the He II spectra is peak 5, which is also visible in the He I spectra, although less intense. This peak increases in intensity at intermediate exposures, but is later reduced at the highest exposures. As seen in the following spectra, a similar peak appears for the [1×1] surface, although less intense, but not for the [1×1];Ni surface. This peak is indicative of the molecular precursor,[11–13] which occurs with variable probabilities on different surfaces even at room temperature. A detailed account of the nature of this state with additional experimental evidences will be published separately in our next paper.[13] Spectra which contain a minimum intensity in peak 5 are obtained by heating the surface to 400 K. Under these conditions the structure disappears, because all precursor molecules are converted to the stable dissociated (atomic) oxygen species.[11,13]

The following figures, Figs. 8 and 9, represent the results for the [1×1] sputter-annealed surface. Positions of peaks and shoulders as well as relative intensities of all oxygen-induced features are identical to those of Figs. 6 and 7 within the error limits indicating that the stable oxygen bond on the [1×1] and [7×7] surfaces is identical or, at least, indistinguishable by UPS. The only exception is peak 5 which is weaker for the [1×1] surface in agreement with the finding that the molecular precursor decays more rapidly on [1×1] than on [7×7].[13]

In Fig. 10, He II spectra from the [1×1;Ni surface are shown. They look generally similar to those from the [7×7] (Fig. 7) and [1×1] surface (Fig. 9), respectively, with some subtle but significant differences. First, the spectrum from the clean surface exhibits a much less pronounced surface (dangling bond) state (peak 2), less intensity in peaks 5 and 8, but a sharper and maybe more intense peak 4, which may contain some Ni 3*d* contribution. Secondly, oxygen adsorption leads to less structure and to less oxygen-induced intensity as compared to spectra from the [7×7] and [1×1] surfaces obtained after the same exposures. This missing intensity is due to a smaller amount of adsorbed oxygen because of the lower sticking coefficient for oxygen on the [1×1];Ni surface

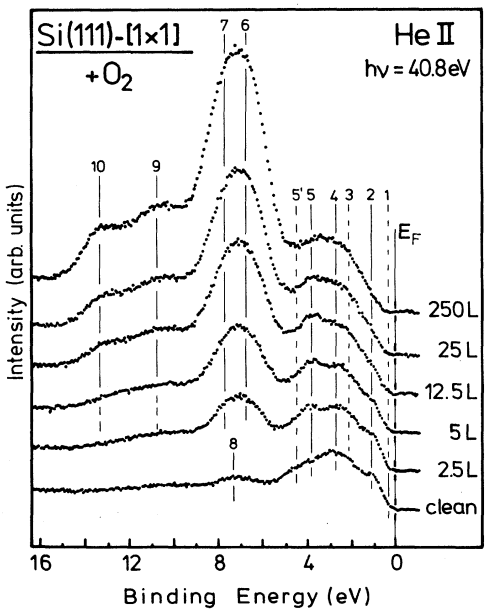

FIG. 9. As Fig. 8 but He II spectra.

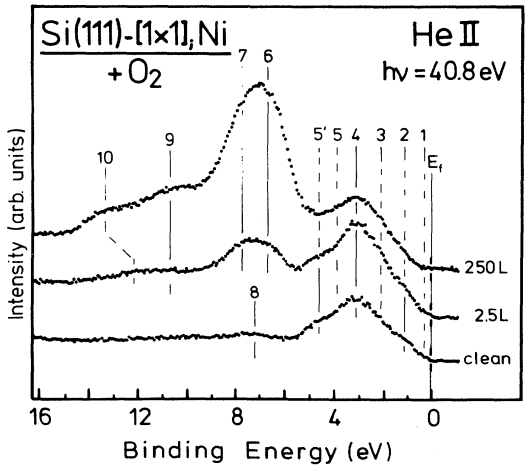

FIG. 10. He II UPS spectra for the clean and oxygen covered Si(111)-[1×1];Ni surface.

(see Sec. IV A). Thirdly, the oxygen-induced peak 5 is missing as no molecular precursor could be observed at room temperature on the [1×1]; Ni surface.[13]

D. XPS valence-band spectra

Figure 11 presents some XPS valence-band spectra obtained with Mg $K\alpha$ radiation for the [7×7] surface and for SiO_2, respectively. We note that the instrumental resolution here is about 0.9 eV as compared to 0.1 eV for He I and 0.3 eV for He II, leading to much broader structures. Due to the different cross section for $h\nu = 1254$ eV the spectra of Fig. 11 look different compared to those of Figs. 6–10 and those of Refs. 5 and 6. In the clean spectrum, peak 4/5 between 3 and 4 eV which is most prominent for He I and He II is hardly seen in Fig. 11, like peak 8 of Figs. 6 and 8. However, a new dominating peak at about 12 eV appears for Mg $K\alpha$ excitation which is most likely due to emission from the bottom of the Si valence band. The relatively high intensity of the 12-eV structure is not unexpected since these bands are mostly derived from Si 3*s* states, and *s* states should have a higher "XPS" cross section than *p* states but a much lower "He I/II" cross section.

The middle spectrum taken after a 250 L O_2 dose is comparable to those obtained with He I or He II under similar conditions. The three peaks at 3.3, 7.6, and 10.3 eV coincide approximately with peaks 4, 6/7, and 9 of Figs. 6–10 (see also Table I). As mentioned, the peak intensities are different due to different cross sections for Mg $K\alpha$ and He I/II. A new, very broad feature between 16 and 32 eV with a maximum at 24.8 eV is also clearly seen in Fig. 11 which is, of course, not observed with He II radiation due to its limited photon energy range.

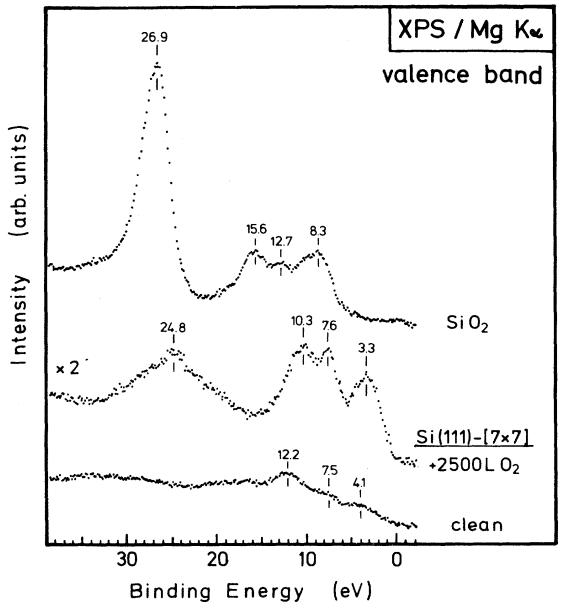

FIG. 11. XPS (Mg $K\alpha$) valence-band spectra from the clean and oxygen covered Si(111)-[7×7] surface and from SiO_2. Note the scaling factor for the middle spectrum.

This peak was also observed in a recent synchrotron study[12] and is due to emission from the O 2*s* level of adsorbed atomic (dissociated) oxygen. Its extraordinary width is not surprising since photoemission from inner valence levels of covalently bound atoms commonly leads to very broad features due to strong electron correlation. This causes configurational mixing and a spreading of the total intensity into very many final states of the photoionized system below and above the expected energy position of the O 2*s* peaks.[28]

Interestingly, the O 2*s* peak becomes much narrower for the SiO_2 sample (topmost spectrum of Fig. 11), more intense, and is shifted only by 2 eV compared to the valence levels which are shifted by 5 eV. Note that apparently all Si-derived peaks (Si 2*p* and valence band) are shifted by 5 eV while the oxygen core levels are shifted only by 2 eV (O 1*s* and O 2*s*). The reason for the relatively large and differential shift is likely to be due to differences in partial charge and differences in "extra-atomic" screening. For example, in the nonconducting silicon oxide sample effective charge-transfer screening is missing. It is remarkable that even the oxygen-derived valence-band peaks behave like Si states (5 eV shift) signaling their partial Si character, whereas the more localized O 2*s* "inner valence" level obviously behaves more like an oxygen core level (2-eV shift) indicating that the O 2*s* level does not significantly contribute to the Si—O bond of SiO_2, in contrast to O/Si. We may speculate that the transition from a more covalent (O/Si) to a more ionic system (SiO_2) is responsible for the observed changes of the O 2*s* peak, leading to quenching of all excited states and hence to the concentration of the total intensity in a "true" O 2*s* peak, i.e., a peak which represents the O 2*s* atomic orbital in a one-electron picture. Perhaps the change of bonding character is also responsible for the apparently enhanced O 2*s* cross section for SiO_2.

Finally, we note that the adsorption of oxygen leads to a gradual lowering of the edge of the valence bands on all the different silicon surfaces studied here (Figs. 6–11), with respect to the Fermi level. This is observed in the spectra as a shift of the onset of emission from the valence band towards higher binding energies. The increase of the negative charge in the surface region is due to donation from the adsorbed oxygen atoms, with the net effect that the bands thereby become flatter than in the initially depleted situation.[29] Under such circumstances sharp structures in the photoelectron spectra should remain sharp, even at higher oxygen coverages. This is the case for the set of spectra obtained here, only counteracted somewhat by effects of surface disorder and scattering.

E. LEED studies

Systematic LEED studies were performed with the [7×7] surface. Patterns of variable quality in terms of contrast and diffuse background were obtained for different levels of C impurities. For the cleanest surface, the changes of the [7×7] pattern were followed for all oxygen exposures included here. We observed that a gradual weakening of the [7×7] pattern and a gradual in-

crease of the diffuse background accompanied the exposure to oxygen. At no point is a new phase, like a [1×1] structure, observed. Most of the long-range order of the [7×7] surface is lost during the fast adsorption stage, which terminates after 12.5 L (see Fig. 12). However, even after very high exposures, e.g., ~10 000 L, parts of the surface still preserve a [7×7] reconstruction, and hence a weak 7×7 overstructure is observed by LEED.

IV. DISCUSSION OF THE ADSORPTION OF THE STABLE OXYGEN SPECIES

A. Oxygen uptake and coverages

Oxygen uptake curves, i.e., coverage versus exposure, of three different Si(111) surfaces are shown in Fig. 12. An absolute coverage scale is given on the right-hand side based on a careful comparison of the present XPS data with those obtained for CO on Ru(001). In that case the saturation coverage corresponds exactly to $\frac{2}{3}$ of a monolayer of CO molecules, under certain conditions.[30] Our comparison was performed under identical experimental conditions taking into account all intrinsic XPS satellites.[31] An overall accuracy of 25% is estimated with the main uncertainty being due to the differences in satellite structures of the O 1*s* lines in these cases. A more extensive discussion of the measurements is given in Ref. 7. Effects of low substrate temperatures will be discussed in our next paper.[13]

The two discernible stages of adsorption illustrated by Fig. 12 were earlier believed to represent or contain different configurations of oxygen.[10,32] It was supposed that the first stage corresponds to chemisorption, leaving oxygen in its stable adsorbed configuration, and that the second stage represented a gradually increasing incorporation of oxygen in a surface oxide.[32] Alternatively, it was suggested that first molecularly bound oxygen adsorbs between two Si atoms of the topmost layer, and then in the "slow sorption stage," dissociation occurs.[33]

From the calibration of coverages, we see that on the [7×7] surface the slow adsorption sets in at a coverage

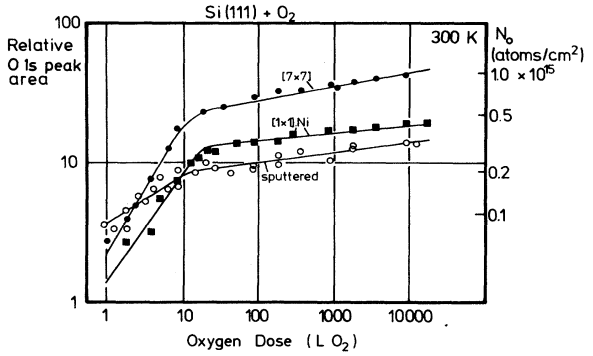

FIG. 12. Oxygen uptake curves derived from O 1*s* data on double-logarithmic scales for three differently prepared surfaces. Note the relative intensity scale (left) and the absolute coverage scale (right) which has been calibrated by careful comparison with the known coverage of CO/Ru(001) (Ref. 30).

of approximately $\frac{1}{2}$ of a monolayer of oxygen atoms with respect to the number of silicon surface atoms (1.12×10^{15} cm^{-2}). We see no differences in XPS or XAES spectra for coverages well below and well above this value. In UPS, the same is true when features due to the precursor are neglected. We therefore conclude that the stable state of oxygen is the same for all coverages studied here, and hence models which postulate differently bound, stable oxygen states in the two sorption regimes appear to be unlikely (see also Sec. IV C).

We further note that the relatively steep initial increase of the uptake curve, i.e., a relatively high sticking coefficient, is most likely due to the occurrence of the observed molecular precursor state as will be discussed later.[13] Here we stress the big influence that surface structure and composition obviously have on the sticking coefficient and the absolute coverages reached for a given exposure. For instance, from Fig. 12 it can be derived that for a 10^4 L O_2 exposure the [7×7] surface adsorbs two times more oxygen than the [1×1];Ni surface, and three times more than the totally disordered (sputtered) surface. This result is somewhat surprising since one usually expects a higher uptake reactivity for the more open surfaces. Qualitatively, one can thus argue that the reconstructed [7×7] surface is in fact more reactive because of relatively many topmost Si atoms in prominent positions[34,35] and because of the relatively large number of dangling bonds. Apparently these are drastically reduced for the [1×1];Ni (compare Figs. 10 and 7), and the sputtered surface.

In the [1×1];Ni case the reason could be that Ni levels hybridize with the surface states thus quenching the dangling bonds and lifting the reconstruction. In the case of the sputtered surface it has been suggested, based on surface extended x-ray-absorption fine structure (SEXAFS) results, that a well-ordered "crystalline" layer of Si atoms is formed on top of the sputter-induced amorphous region.[36] In this layer, rearrangement of surface atoms with optimum saturation of Si bonds is likely to occur and hence neither free dangling bonds nor prominent Si atoms are expected to facilitate the oxygen uptake and dissociation. Our result (Fig. 12) is thus compatible with the finding of the SEXAFS study.[36]

B. Local bonding of the stable state

The configuration of the stable state of adsorbed oxygen can be derived from the combined experimental evidence presented above, and from a comparison with theoretical predictions for different stucture models. The different electron spectroscopies and ion probes, that have been applied to study this system, have different sensitivities to the structure of oxygen. The electronic states are probably best studied by UPS and synchrotron radiation-induced photoemission at low (<200 eV) photon energies. Typical early results of such studies[37] showed strong oxygen-derived peaks to dominate the spectra obtained with He I and He II light sources. Evidence for the involvement of the dangling bonds (on cleaved surfaces) in the adsorption process was obtained even earlier.[38,39]

The quality of UPS data remained relatively unchanged for about a decade, with several reports of the features in UPS spectra corroborating the early data. In view of this, theoretical calculations of local densities of states were performed to explain the UPS results[8,40–42] testing atomic and molecular bonding geometries. Agreement between these theories and *any* of the experiments was never quite satisfactory, as the calculated densities of states were never matched by the same details in the experimental data. The present set of data represents an improvement of this situation, as illustrated by Figs. 6–10. Here the main oxygen related structure at about 7.5 eV is clearly resolved as two peaks with different symmetry, and the photoelectron distributions in general show clearly identifiable peaks and shoulders.

The models for the configuration of adsorbed oxygen fall into two classes, molecularly adsorbed and dissociated, i.e., atomic oxygen. For the stable state discussed here, all the present evidence (XPS O 1*s*, XAES, and UPS data, see Sec. III, as well as the molecular precursor[11–13]) speaks in favor of a dissociated, atomic configuration. For the UPS data this is now discussed in more detail.

Different positions of the oxygen atom have recently been examined, in Ref. 8 including monatomic on-top (of the dangling bond) and bridge-bonded positions. Calculated valence orbital energies and populations[8] are compared to our UPS spectra in Fig. 13. The on-top position in the upper panel of Fig. 13 disagrees with the present experiments, since it predicts a single (O_π) oxygen-derived peak and only one more peak (O_σ) at slightly higher binding energy, in contrast to the double-peak structures 6/7 and 9/10. Moreover, neither peak 9, which is only observed for *s* polarization, nor peak 7, which is equally intense for both polarizations, is compatible with an O_σ band since such σ states should be totally symmetric with respect to the Si-O axis which coincides with the surface normal in this case; hence the σ bands for the on-top position should be observed only for *p* polarization, in disagreement with the results of Figs. 6 and 13.

Similar arguments can be used to exclude double-bonded (diatomiclike) Si=O with oxygen in on-top position, as suggested by Ludeke and Koma[43] and recently for a minority species by Hollinger *et al.*[6] and Schell-Sorokin and Demuth.[3] In this case, peak 9 must also represent a σ-like bond, namely, that which is equivalent to the 4σ orbital (or $4a_1$ in C_{2v} symmetry) of the analoguous organic carbonyls, or adsorbed CO, and peaks 6 and 7 would be due to 5σ ($5a_1$) and 1π ($1b$) orbitals. Again, the polarization dependence shown in Figs. 6 and 13 is incompatible with such an assignment, in agreement with chemical intuition which suggests that double-bonded Si=O species would not be stable under the present conditions.[44]

A much better agreement is offered by assuming the bridging position connecting silicon atoms in the first and second layer as either a single bridge or as two bridges per surface unit cell. This would assign peak 6 as the O_π level and peak 7 as the O_i level, having different symmetries, as indeed observed for the [7×7] surface with *s* and *p* polarized light. Peaks 9 and 10 should then have O_σ character, although the energies predicted for these peaks are somewhat higher than observed, which is not surprising in view of the model character of such calculations[8] and in view of the unknown geometrical parameters. The local symmetry of the bridge position would be C_{2v}. For this symmetry group the nonbonding O($2p$) electrons should mainly contribute to the $2b_1$ and $7a_1$ orbitals,[25] and the bonding O($2p$) electrons to the $5b_2$ orbital. The $2b_1$ orbital should be oriented perpendicular to the plane containing the oxygen and silicon atoms, i.e., it lies approximately in the surface plane. It should be totally nonbonding like the O_π band of Ciraci *et al.*[8] and should be visible preferentially with *s* polarization, in agreement with the observed behavior of peak 6. The $7a_1$ orbital lies in the SiO-Si plane, is weakly bonding like the O_i band of the slab calculation, and should be observable with *s* as well as with *p* polarization, in agreement with the dependence of peak 7. Finally, the bonding $5b_2$ orbital, which is antisymmetric with respect to the symmetry axis in C_{2v} symmetry, and which should be equivalent to the O_σ band in the model of Ciraci *et al.*, is expected to be predominantly observable with *s* polarization, like peak 9 of Figs. 6 and 13.

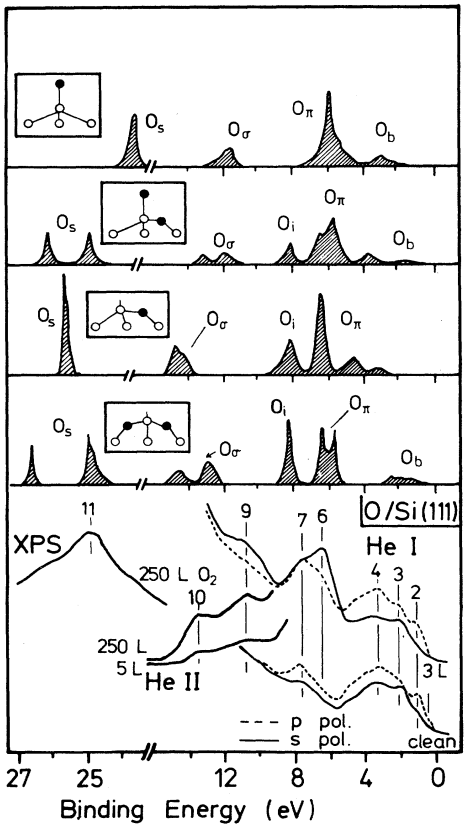

FIG. 13. Comparison of experimental He I, He II, and XPS valence-band data from oxygen covered Si(111)-[7×7] (taken from Figs. 6, 7, and 11) with the results of theoretical calculations by Ciraci *et al.* (Ref. 8) for four different adsorbate configurations as indicated in the figure.

The He II spectra (Figs. 7, 9, and 10) have shown that after exposures of 5 L O_2, or more, peak 9 splits into two peaks labeled 9 and 10. This is also in excellent agreement with the results of the calculations of Ciraci *et al.* which yielded a splitting of the O_σ band when, at higher coverages, two oxygen atoms become bonded to one Si atom in the topmost layer (see also Fig. 13). The simultaneous splitting of the O_π peak would not be resolvable by our measurements. However, the predicted occurrence of two O 2*s* peaks at higher coverages is not seen in our data (see Fig. 11). The reason is likely that the calculation overestimated the delocalized valence-band character of O 2*s* derived states, which presumably are more localized, corelike in this case. Hence less, or no, splitting is expected which, together with the correlation effects expected for inner valence levels,[28] would be compatible with the broad O 2*s* feature of Fig. 11.

In conclusion, the UPS results clearly favor the assignment of dissociated, bridge-bonded oxygen as the *major* stable product of the chemisorption reaction. Of course, we cannot completely exclude that a minority species (e.g., less than 10%) of on-top oxygen also exists; this is discussed in Sec. IV C in more detail. Also, a minority of bridging atoms in unfavorable bonding configurations (as discussed at the end of Sec. IV C) which may lead to some smearing of UPS structures cannot be excluded. The Si 2*p* and O 1*s* spectra, and the UPS data, show that the majority species of adsorbed oxygen has very little influence on the surface charge distribution, and that a single species of oxygen dominates over the whole range of coverages studied here. The influence of this species on the dangling bond states is relatively small, as seen in the UPS spectra. This observation further corroborates the finding of an oxygen position between Si atoms of the first and second layer, respectively, since oxygen breaks a backbond in this model leaving the dangling bonds essentially unaffected. The disappearance of the sharp dangling bond peaks in the cases of high oxygen coverages ($\gg 12.5$ L) is mainly an effect of the disorder of the surface, as measured with LEED. From the O *KLL* spectra, compared empirically with a selection of various experimental results from other relevant oxygen configurations, an atomically bonded oxygen configuration is also clearly indicated. We note at this point that a similar configuration of oxygen was already suggested by Ibach *et al.*[4] based on systematic HREELS studies.

C. Discussion of an on-top minority species

Recently Hollinger *et al.*[6] suggested the presence of two chemisorbed oxygen states for room temperature (RT) adsorption in the low-to-medium coverage range ($1-10^4$ L O_2), based on the finding of an asymmetric O 1*s* peak. Their conclusion is in agreement with that of Schell-Sorokin and Demuth[3] but different from that of Ibach *et al.*,[4] the last two based on low-temperature HREELS results. Hollinger *et al.* identified one major O 1*s* component (80% of total oxygen coverage) as bridging, oxidelike oxygen, as in the present study, and one minor component (20%) as nonbridging, diatomiclike monoxide. In our previous[7] and in the present study (see Figs. 3 and 4) we also observed a shoulder on the high binding-energy side of the O 1*s* peak but come to a different assignment. Hollinger *et al.* also give three supporting arguments, the disappearance of the shoulder upon annealing at 500 °C, a charge-transfer argument to explain the binding-energy shift, and the mentioned interpretation of Schell-Sorokin and Demuth.[3] Their diatomiclike interpretation of the minority species in the O 1*s* spectra has very recently been adapted by other authors (see, e.g., Ref. 21). We disagree with this interpretation for the following reasons.

(1) Our XPS O 1*s* data do not show an angular dependence (see Sec. III A); in particular, the intensity ratio of shoulder and main peak is constant for all angles, even for grazing exit angles for which the surface sensitivity is highest. If the shoulder would be due to a diatomiclike monoxide it should be enhanced for grazing exit angles as this species is expected to be located in the topmost layer[6] as compared to the main bridge-bonding species which occupies sites between first- and second-layer Si atoms.

(2) The O 1*s* spectra from a sputtered surface do not (or hardly) contain a shoulder at the high-BE side of the oxygen peak (Fig. 4) although all other data are identical to those from the [7×7] reconstructed surface. Such behavior is unlikely if the shoulder were due to an additional species.

(3) The Auger data are *not* compatible with a diatomic on-top oxygen species. Since such an oxygen adsorbate should yield a rather different Auger fine structure compared to the bridging species (e.g., one which is similar to that of isoelectronic adsorbed carbon monoxide[3]) at least a few of its peaks or shoulders should be clearly distinguishable from those of the majority (bridging) oxygen. A careful analysis of the Auger line shapes, however, excludes the presence of such an additional species if it contributes more than about 10% to the total oxygen coverage. Note that the Auger fine structures can be a very sensitive tool for the distinction of chemical states, in particular for covalent bonds.[23,24]

(4) The UPS data are also incompatible with two different oxygen species. Neither in our data nor in the data of Hollinger *et al.*[6] can additional peaks or shoulders be found that disappear upon annealing at 500 °C. However, additional structures are expected for an on-top minority species such as a diatomiclike monoxide. Moreover, all observed peaks are well explained by the calculations of Ciraci *et al.*[8] for bridging oxygen but are incompatible with an on-top adsorbate (see preceding section).

(5) We also disagree with Schell-Sorokin and Demuth's interpretation of the additional HREELS peaks,[3] as discussed in detail elsewhere,[12] since we found features of a precursor state at the low-BE side of the main O 1*s* peak (and in UPS, near-edge x-ray-absorption fine-structure spectroscopy, and XAES) which is unambiguously due to a molecular adsorbate state and explains the additional HREELS peak. This finding is in agreement with the interpretation of Ibach *et al.*[4] who observed the same HREELS structure, as shown in Ref. 3, and assigned it to a molecular state. These authors also argued that a vibrational frequency identical to that of an isolated Si=O molecule (as found for the additional HREELS

peak) appears to be unlikely for a diatomiclike adsorbate due to the presence of Si backbonds.

As we clearly exclude the interpretation of two dissociated, rather different adsorbate states for the observation of an asymmetric O 1*s* peak, we should offer an alternative explanation. In our opinion the most likely interpretation is that of excitonic and/or interband excitations which accompany the main O 1*s* and Si 2*p* peaks as satellites and appear with significant intensity under certain conditions. This idea is discussed in more detail in Sec. IV D. However, we cannot exclude that the main origin of the asymmetric O 1*s* structure is simply the inhomogeneity of oxygen adsorbate bonds. It is conceivable that the squeezing of oxygen atoms into an ordered surface layer leads to distorted Si-O-Si bridges, unfavorable bond distances, or even unsaturated bonds. Hence a distribution of electronic bonding configurations which slightly differ from each other may result.

Arguments for such an explanation can be found in all spectroscopic results. For example, upon annealing the O 1*s* asymmetry disappears and all adsorbate-induced structures in the UPS and HREELS spectra become sharper.[3,6] This is consistent with the experience that annealing usually causes a spatial and electronic rearrangement of adsorbate bonds thus leading to a relaxation of bond distortions and to a homogeneous distribution of the energetically favorable oxygen bond which is apparently the Si-O-Si bridge configuration. Such a model is also consistent with a redistribution of Si 2*p* satellite intensity upon annealing,[6] and with the fact that the best ordered [7×7] surface shows the highest O 1*s* satellite intensity while the disordered sputtered surface shows the weakest (Fig. 4). Indeed, the better ordered the clean surface is the more stress and distortion is expected to occur upon incorporation of oxygen.

D. Alternative interpretation of satellite structures

As mentioned in Sec. III A and in the preceding section we do not believe that there is presently an unambiguous, completely satisfactory explanation for the additional oxygen-induced core-level structures or satellites. In general, structure at the high-BE side of a peak could have at least three different types of origins.

First, *inelastic losses* occur on the low-kinetic-energy (KE) side of a peak. They can have discrete energies, like plasmons or excitations from occupied to unoccupied orbitals or bands, or they contribute to a widespread structureless enhancement of the background. The lack of pronounced peaks and the increase of the additional Si 2*p* features at grazing exit angles could support such an interpretation. However, there are clear arguments against this interpretation from the fact that for photon energies close to threshold or for normal emission from a surface layer of adsorbed oxygen a similar structure is observed as well as from the observation that the additional Si 2*p* structure is limited to a very small energy range (about 3.5 eV) below the Si 2*p* level.

Secondly, *intrinsic losses or excitations,* i.e., excitations which occur together with and are coupled to the photoionization process, could be observable in photoemission experiments from solids or adsorbates. Such excitations could be plasmons, shake-up processes, interband transitions, excitons, etc. While plasmons in Si require excitation energies ($\Delta E_{\text{volume}} \sim 18$ eV, $\Delta E_{\text{surf}} \sim 12$ eV) much higher than the "loss" energy observed, and shake-up processes usually occur only in free molecules[45] and in molecular solids or adsorbates,[31] interband transitions and/or excitons are conceivable candidates as explanation for the low-KE structures of Figs. 1–4. They will be discussed below.

Chemical shifts are the third possible explanation for the structures at higher binding energies. In fact, as mentioned and discussed in the preceding section Hollinger and Himpsel[5,15] interpreted their Si 2*p* and O 1*s* spectra in such a way. This interpretation is supported by the appearance of prominent peaks at 4.5 eV (Si $2p_{3/2}$) and ~2 eV (O 1*s*) higher binding energies (see Figs. 2 and 3) when SiO_2 layers are formed, and by the structures between the Si 2*p* peaks of pure Si and SiO_2, respectively, which were observed for thin silicon oxide layers thermally grown on a pure Si substrate.[5,19] The question is, however, whether *small amounts* of adsorbed oxygen in the (sub)monolayer range, as studied here, already lead to the formation of Si^{+}-, Si^{2+}-, Si^{3+}-, Si^{4+}-like states which give rise to discernible peaks in the Si spectra. We have serious doubts, and hence we suggest interband and excitonic excitations as an alternative explanation. This will now be discussed.

First to the doubts: As mentioned above, our Si 2*p* peaks at higher binding energies, apart from that at 0.9 eV, are barely discernible and not reproducible in different spectra which would be surprising if they represent different Si^{n+} states. Of course, multiple bond configurations such as those discussed in Sec. IV C (bond distortion, disorder, etc.) can cause a smearing of structures. However, in this case the sharp peak at 0.9 eV would be at variance. Secondly, it appears unlikely that oxygen coverages far less than a monolayer should already lead to Si^{3+} and Si^{4+} states. Thirdly, the Si 2*p* structure at higher BE increases as a whole for successively increasing oxygen coverages as seen in Fig. 2. However, if discernible Si^{n+} states exist, we would expect to observe first the appearance of Si^{1+}, then Si^{2+}, etc., since, on the average, Si atoms in the surface region will first react with one oxygen, then with two, etc. Fourthly, there is only one major O 1*s* peak with an increasing but small shoulder at higher binding energy for all O coverages studied here. This indicates that the O 1*s* binding energy is insensitive to the state of the neighboring Si atom(s) since most of the intensity is concentrated in only one O 1*s* peak for low as well as for high coverages. However, the O 1*s* shoulder then remains to be explained. In the chemical-shift picture it must represent oxygen either in a different chemical state (which was excluded in Sec. IV C), or in distorted bonds (which would be somewhat surprising in the light of the insensitivity to the state of the Si neighbors), or bound to Si^{4+} because it appears at the same energy as oxygen in SiO_2 (see Fig. 3), and because Si^{4+} is the only minority Si species expected in this exposure range. But why should only Si^{4+} neighbors cause a shift of the O 1*s* level and not Si^{3+} or Si^{2+}?

Fifthly, the absence of an O 1*s* shoulder in the case of the sputtered surface (Fig. 4) remains unexplained (no Si^{4+}?). Sixthly, annealing at 500 °C causes a significant reduction of "Si^{1+} and Si^{2+}" while no equivalent increase of Si^{3+} and Si^{4+} peaks is observed.[6]

These inconsistencies and our experience with satellites in adsorbate systems[31] have lead us to the suggestion that in the *low-coverage range* studied in this work, the additional structures in the Si 2*p* and O 1*s* spectra are due to excitonic and interband excitations rather than to chemically shifted states. We suggest that the peak at 0.9-eV higher BE is due to an excitonic "shake-up" process in which, in addition to the normal photoemission process, an electron is excited from the top of the valence band to an excitonic level in the band gap. From the energy position of this peak we derive that the binding energy of the exciton is about 0.2 eV as measured from the bottom of the conduction band. This value is within the range of older experimental results [0.15–0.9 eV (Ref. 46)] which lead to a long-standing controversy because of their large discrepancy ($\sim$0.7 eV). Recent experimental[47] as well as theoretical[48] results, however, converge towards an exciton binding energy of 0.2 ± 0.15 eV which is in perfect agreement with our Si 2*p* satellite. We note, however, that most published results refer to a core excitation, i.e., a transition $2p \rightarrow$ excitonic level, whereas in our picture two holes were created, one in the photoionized 2*p* level and one in the valence band. It is not clear yet whether the valence-band hole stays localized due to the presence of the 2*p* hole and hence contributes to a higher binding energy of the exciton, or whether the influence of the valence-band hole is negligible because of delocalization.

The structure at higher binding energy could be due to interband (shake-up) transitions, i.e., to excitation of an electron from the valence to the conduction band simultaneous with the 2*p* photoionization. In this case the "loss" structure should be similar to the convolution of valence and conduction band weighted by an overlap matrix element. This weighted convolution should result in a broad hump with only little structure and a 1.1 eV separation from the main peak, which is consistent with our experimental observation for both core levels. The assertion that interband (or excitonic) transitions in the Si substrate contribute to the O 1*s* adsorbate spectrum is corroborated by similar findings for adsorbed oxygen, nitrogen, or carbon atoms on metal surfaces.[31]

Finally the question remains to be answered, why excitonic and interband excitations only appear in the presence of oxygen. Hjalmarson *et al.*[49] pointed out that for the Si 2*p* level the predicted Frenkel core exciton should have a negative binding energy, i.e., it becomes a conduction-band resonance, because the Si $(Z+1)$ analogue, phosphorus, is a shallow donor in Si. It appears plausible that neither the resonant Frenkel nor the bound but delocalized Wannier exciton have sufficient overlap with the Si 2*p* core level in order to contribute to a significant shake-up intensity. Hjalmarson *et al.* also argued that only a slightly more attractive central-cell potential would be necessary for a localized Frenkel-type exciton. We suggest that such a change of the Si potential is induced by bonding oxygen neighbors, and hence localized Frenkel excitons are enabled by the presence of oxygen. A similar effect, namely, an enhanced central-cell potential and hence a contraction and localization of the wave function of the valence and conduction electrons, could also be responsible for the increase of the interband transitions induced by adsorbed oxygen. However, this is speculation at present.

In conclusion of this section we feel that there are convincing reasons to reject the chemical-shift picture for the additional structure at the high binding-energy side of Si and O core levels for room-temperature adsorption in the *monolayer regime.* Instead, we suggest that excitonic and interband excitations are responsible for the observed structures in the XPS spectra. We stress that the findings discussed above can easily be understood within an excitation model. For heavily oxidized samples, or for thin, thermally grown Si/SiO_2 interfaces, the chemical-shift picture is still applicable since experiments in these cases show much higher intensities and clearly discernible peaks in the high-BE range.[5,19]

V. SUMMARY

Based on the combined use of various spectroscopies such as high-resolution XPS (Si 2*p*, O 2*s*, *and* O 1*s*), XAES, and, in particular, polarization-dependent UPS data we have obtained a rather complete set of spectroscopic information under identical conditions on differently prepared Si(111) surfaces, at room temperature and at low-to-medium coverages. The UPS results are compared to, and agree very well with, theoretical calculations.

Thus we arrive at a consistent interpretation of the configuration of the stable chemisorbed oxygen species. This species is an oxygen atom inserted in the lattice in bridging positions between silicon atoms in the first and second layer, respectively. It occurs from the lowest coverages up to a full monolayer coverage, and probably at higher coverages, too.

This stable species is preceded by a molecular adsorption state, which occurs with variable lifetimes and intensities on differently prepared surfaces and under differing experimental conditions, as described in Refs. 11 and 12 and in the following paper.[13]

The presence of a second dissociated stable oxygen state for RT adsorption (e.g., a nonbridging, diatomiclike monoxide) is clearly excluded by our data.

The additional Si 2*p* and O 1*s* structures on the high binding-energy side of the main peaks can be understood in the framework of the conventional chemical shift model, but a new interpretation which appears more likely is suggested for adsorption in the *monolayer regime.* In this new model the structures are explained as satellites arising from excitonic and interband transitions that preferentially occur on well-ordered surfaces after adsorption of some oxygen.

ACKNOWLEDGMENTS

One of the authors (P.M.) expresses his gratitude to Technische Universität München for support and hospi-

tality, particularly to D. Menzel and F. Koch. G. Abstreiter kindly provided the silicon samples. Discussions with G. V. Hansson, J. Onsgaard, S. Tougaard, W. Göpel, E. Bauer, C. Y. Su, I. Lindau, D. R. Jennison, and D. E. Ramaker are gratefully acknowledged. This project is supported by Deutsche Forschungsgemeinschaft (Sonderforschungsbereich-128), and by Odense University, Denmark.

---

*Permanent address: Fysisk Institut, Odense Universitet, Campusvej 55, DK-5230 Odense M, Denmark.

†Present address: Physikalisches Institut, Universität Stuttgart, D-7000 Stuttgart 80, West Germany.

[1]C. W. Wilmsen, J. Vac. Sci. Technol. **19**, 279 (1981).

[2]G. Landgren, R. Ludeke, Y. Jugnet, J. F. Morar, and F. J. Himpsel, J. Vac. Sci. Technol. B **2**, 351 (1984).

[3]A. J. Schell-Sorokin and J. E. Demuth, Surf. Sci. **157**, 273 (1985).

[4]H. Ibach, H. D. Bruchman, and H. Wagner, Appl. Phys. A **29**, 113 (1982).

[5]G. Hollinger and F. J. Himpsel, Appl. Phys. Lett. **44**, 94 (1984).

[6]G. Hollinger, J. F. Morar, F. J. Himpsel, G. Hughes, and J. L. Jordan, Surf. Sci. **168**, 616 (1986).

[7]P. Morgen, W. Wurth, and E. Umbach, Surf. Sci. **152/153**, 1086 (1985).

[8]S. Ciraci, E. Ellialtioglu, and S. Erkoc, Phys. Rev. B **26**, 5716 (1982).

[9]See, e.g., D. V. Mc Caughan and J. C. White, in *Handbook of Semiconductors*, edited by C. Chilsum (North-Holland, Amsterdam, 1981), Chap. 3 A.

[10]J. T. Law, J. Phys. Chem. Solids **4**, 91 (1958); M. Green and K. H. Maxwell, J. Phys. Chem. **1**, 145 (1960).

[11]U. Höfer, P. Morgen, W. Wurth, and E. Umbach, Phys. Rev. Lett. **55**, 2979 (1985).

[12]U. Höfer, A. Puschmann, D. Coulman, and E. Umbach, Surf. Sci. (to be published).

[13]U. Höfer, P. Morgen, W. Wurth, and E. Umbach (unpublished).

[14]C. M. Garner, I. Lindau, C. Y. Su, P. Pianetta, and W. E. Spicer, Phys. Rev. B **19**, 3944 (1979).

[15]G. Hollinger and F. J. Himpsel, Phys. Rev. B **28**, 3651 (1983).

[16]M. T. Anthony and M. P. Seah, Surf. Interface Anal. **6**, 95 (1984); **6**, 107 (1984).

[17]U. Höfer, Diplomarbeit, Technical University München, 1985.

[18]P. J. Grunthaner, M. H. Hecht, F. J. Grunthaner, and N. M. Johnson, J. Appl. Phys. **61**, 629 (1987).

[19]W. Braun and H. Kuhlenbeck, Surf. Sci. **180**, 279 (1987).

[20]A. Franciosi, P. Soukiassian, P. Philip, S. Chang, A. Wall, A. Raisanen, and N. Troullier, Phys. Rev. B **35**, 910 (1987).

[21]K. Uno, A. Namiki, S. Zaima, T. Nakamura, and N. Ohtake, Surf. Sci. **193**, 321 (1988); A. Namiki, K. Tanimoto, T. Nakamura, N. Murayama, and T. Suzaki, *ibid.* (to be published).

[22]W. E. Moddeman, T. E. Carlson, M. O. Krause, B. P. Pullen, W. E. Bull, and G. K. Schweitzer, J. Chem. Phys. **55**, 2371 (1971).

[23]J. C. Fuggle, E. Umbach, R. Kakoschke, and D. Menzel, J. Electron Spectrosc. Relat. Phenom. **26**, 111 (1982).

[24]C. T. Chen, R. A. DiDio, W. K. Ford, E. W. Plummer, and W. Eberhardt, Phys. Rev. B **32**, 8434 (1985); W. Wurth, C. Schneider, R. Treichler, E. Umbach, and D. Menzel, *ibid.* **35**, 7741 (1987); *ibid.* **37**, 8725 (1988).

[25]D. E. Ramaker, J. S. Murday, N. H. Turner, G. Moore, M. G. Lagally, and J. Houston, Phys. Rev. B **19**, 5375 (1979).

[26]F. J. Himpsel, D. E. Eastman, P. Heimann, B. Reihl, C. M. White, and D. M. Zehner, Phys. Rev. B **24**, 1120 (1981).

[27]R. I. G. Uhrberg, G. V. Hansson, U. O. Karlsson, F. M. Nicholls, P. E. S. Persson, S. A. Flodström, R. Engelhardt, and E.-E. Koch, Phys. Rev. B **31**, 3795 (1985).

[28]See, e.g., L. S. Cederbaum, W. Domcke, J. Schirmer, and W. von Niessen, *Advances in Chemical Physics*, edited by I. Prigogine and S. A. Rice (Wiley, New York, 1986), Vol. 65, p. 115.

[29]A. Many, Y. Goldstein, and N. B. Grover, *Semiconductor Surfaces* (North-Holland, Amsterdam, 1971).

[30]H. Pfnür and D. Menzel, J. Chem. Phys. **79**, 2400 (1983).

[31]E. Umbach, Surf. Sci. **117**, 482 (1982).

[32]F. Meyer and J. J. Vrakking, Surf. Sci. **38**, 275 (1973), and references therein.

[33]M. Green and A. Liberman, J. Phys. Chem. Solids **23**, 1407 (1962).

[34]See, G. Binnig, H. Rohrer, Ch. Gerber, and E. Weibel, Phys. Rev. Lett. **50**, 120 (1983); E. G. McRae, Surf. Sci. **147**, 663 (1984); R. Tromp and E. J. van Loenen, Phys. Rev. B **30**, 7352 (1984); R. Keim, Doctoral thesis, Technische Hogeschool, Twente, Enschede, The Netherlands, 1986.

[35]K. Takayanagi, Y. Tanishiro, S. Takahashi, and M. Takahashi, Surf. Sci. **164**, 367 (1985); G. X. Qian and D. J. Chadi, J. Vac. Sci. Technol. A **5**, 906 (1987).

[36]F. Comin, L. Incoccia, P. Lagarde, G. Rossi, and P. H. Citrin, Phys. Rev. Lett. **54**, 122 (1985).

[37]J. E. Rowe and H. Ibach, Phys. Rev. Lett. **32**, 421 (1974).

[38]L. F. Wagner and W. E. Spicer, Phys. Rev. Lett. **28**, 1381 (1972).

[39]D. E. Eastman and W. D. Grobman, Phys. Rev. Lett. **28**, 1378 (1972).

[40]W. A. Goddard III, A. Redondo, and T. C. McGill, Solid State Commun. **18**, 981 (1976).

[41]M. Chen, I. P. Batra, and C. R. Brundle, J. Vac. Sci. Technol. **16**, 1216 (1979); P. Batra, P. S. Bagus, and K. Hermann, Phys. Rev. Lett. **52**, 384 (1984).

[42]T. Kunjunny and D. K. Ferry, Phys. Rev. B **24**, 4593 (1981).

[43]R. Ludeke and A. Koma, Phys. Rev. Lett. **34**, 1170 (1975).

[44]A. F. Holleman and E. Wiberg, *Lehrbuch der anorganischen Chemie* (De Gruyter, Berlin, 1976), p. 531.

[45]See, e.g., T. A. Carlson, *Photoelectron and Auger Spectroscopy* (Plenum, New York, 1975).

[46]F. C. Brown and O. P. Rustgi, Phys. Rev. Lett. **28**, 497 (1972); W. Eberhardt, G. Kalkoffen, C. Kunz, D. E. Aspnes, and M. Cardona, Phys. Status Solidi B **88**, 135 (1978); R. S. Bauer, R. Z. Bachrach, D. E. Aspnes, and J. C. McMenamin, Nuovo Cimento **39B**, 409 (1977); G. Margaritondo and J. E. Rowe, Phys. Lett. **59A**, 464 (1977).

[47]G. Margaritondo, A. Franciosi, N. G. Stoffel, and H. S. Edelman, Solid State Commun. **36**, 297 (1980).

[48]K. E. Newman and J. D. Dow, Solid State Commun. **50**, 587 (1984); S. Krishnamurthy, A. Sher, and A. B. Chen, Phys. Rev. Lett. **55**, 320 (1985).

[49]H. P. Hjalmarson, H. Büttner, and J. D. Dow, Phys. Rev. B **24**, 6010 (1981).